



## Development of Airport Pavement Condition Evaluation Using Dominant Damage and Grid-Based Analysis

Aris Wibowo<sup>1\*</sup>, Ade Sjafruddin<sup>1</sup>, Bambang S. Subagio<sup>1</sup>, Russ Bona Frazila<sup>1</sup>

<sup>1</sup> Faculty of Civil and Environmental Engineering, Bandung Institute of Technology, Bandung, West Java, 40132, Indonesia.

Received 28 November 2024; Revised 25 March 2025; Accepted 03 April 2025; Published 01 May 2025

### Abstract

Airport Pavement Condition Index (PCI) is a measure of pavement stability represented by an index ranging from 0 (failed) to 100 (best). The PCI evaluation procedure includes a series of steps, which are time-consuming and expensive. Therefore, this study aimed to propose an alternative PCI evaluation procedure that focused on major pavement damage using a grid-based system. The methods used in the analysis included discussions with expert panels and linear & nonlinear regression analysis. The results of the deduct value curve showed good statistical performance with an average RMSE of 1.80 and an average  $R^2$  value of 0.85. The sample unit size with a grid system of  $3 \times 5$  m<sup>2</sup> produced good accuracy with an average standard deviation of 7.89 at the study locations of PKY, TJQ, and TKG airports. Additionally, the PCI value decline model as a function of pavement age produced an estimated PCI decline of 3.23 per year. Grid-based PCI analysis was further proven to improve the accuracy of PCI values and consequently increased the efficiency of runway condition investigation time and costs by 27.30% compared to standard methods. Future studies were recommended to integrate this PCI evaluation procedure with a classification algorithm for airport pavement damage.

**Keywords:** Pavement Condition Index; Deduct Value; Pavement Damage; Grid-Based Analysis.

### 1. Introduction

In 2024, Indonesia records 251 airports spread across the country, with a total domestic air transportation volume of 65.95 million passengers transported through 518,399 aircraft movements. Furthermore, international flights in 2023 account for 9.19 million passengers, with total aircraft departures reaching 178,196 movements (Kemenhub, 2024). Managing many airports poses a challenge for the country, considering the critical role of air transportation in regional development and economic growth.

A study in China including a system of 235 airports shows a positive impact on the economic sector and regional development in cities served significantly by airports. Additionally, the positive impact is felt by the surrounding cities connected to the airport [1]. Economic and urban development driven by airport construction also influences regional disparities. In China, airports built in eastern, central, and northern regions reduce disparities in surrounding cities relative to the national average. In contrast, airports in the western region primarily reduce disparities within the host city without significantly impacting nearby cities [2]. Another study conducted using a nighttime light intensity method for 13,038 cities worldwide provided new evidence that airport construction had a good economic impact. This is shown by a nighttime light increase of up to 10.8% in cities with low initial light intensity and 9.5% in cities gaining new airports for the first time [3].

\* Corresponding author: 35021307@mahasiswa.itb.ac.id

 <http://dx.doi.org/10.28991/CEJ-2025-011-05-011>



© 2025 by the authors. Licensee C.E.J, Tehran, Iran. This article is an open access article distributed under the terms and conditions of the Creative Commons Attribution (CC-BY) license (<http://creativecommons.org/licenses/by/4.0/>).

Airport systems can generally be divided into two, namely, the airside and the landside. On the airside, key facilities include runways, taxiways, and aprons, which are generally constructed using either flexible or rigid pavements. The function of the runway is crucial because it is the landing and take-off area for aircraft. The condition of the runway pavement also affects the level of safety during landing and take-off. In runway conditions with damaged pavement in the form of rutting, standing water often occur when it rains. Aircraft landing on a runway with a water layer thickness of 8 mm requires 1.6 times longer braking time than a dry runway. The distance needed for an aircraft in these conditions reaches 5.3 times longer than a dry runway [4]. Standing water on airport runways can also cause hydroplaning phenomena, reducing wheel grip when landing in the rainy season [5]. Several other studies have shown the importance of maintaining pavement conditions to improve flight safety. Runway pavement is managed by routine and periodic maintenance through the airport pavement management system (APMS).

APMS is a very useful method that includes procedures for collecting, analyzing, storing, and reporting data to support airports in determining the optimum solution with lower costs to maintain pavement assets [6]. This process includes the collection, evaluation, and prediction of pavement condition data; estimating costs for maintenance strategies; and identifying optimal maintenance scenarios. At certain stages of APMS implementation, a thorough investigation of the current pavement conditions can be carried out to evaluate errors caused during the analysis process [7]. The investigation results are the basis for airport managers to decide pavement maintenance scenarios.

Decision-making on airport runway investment is carried out by considering various criteria, including economic, technical, environmental, and social. Technical criteria consist of pavement conditions and the integrity of pavement structures [8]. Airport pavement conditions are generally based on surface condition assessments. However, other parameters can be considered, such as the level of pavement damage (D%), bearing capacity (N%), roughness (As%), unevenness (R%), and surface tensile strength (Wod%), which further require field and laboratory testing [9]. Data collection for pavement condition assessments is also collected by conducting visual observations of airport pavements. Observations of pavements at airports are limited by window time, specifically at airports with a high number of aircraft movements.

To address this limitation, several methods are carried out, including conducting observations using vehicles. A study at Amilcar Cabral International Airport in Sal Island, Cape Verde, showed that vehicle-based observations produced results consistent with direct visual inspections [10]. Besides vehicles, drone observations of airport pavement conditions are also examined. This study was conducted at Aardvark Airfield, the United States Air Force Academy (USAFA) in Colorado Springs. The runway surface condition snapshots are further analyzed using an artificial intelligence method to predict damage. Predictions of the damage type are input into calculating the pavement condition index. The method has successfully shown that collecting data with drones and processing using artificial intelligence has positive results as an alternative to manual pavement condition calculations [11]. These various methods aim to achieve accurate and reliable assessments of pavement conditions.

Pavement conditions are represented by the PCI, a quantitative measure ranging from 0 (worst condition) to 100 (best condition). The PCI value is determined through a procedure including visual field observations of up to 16 types of pavement damage, categorized into three levels, namely low, medium, and high. Based on the damage information collected in the field, a deducted value (DV) is determined as a function of the damage density in a sample area of 450 m<sup>2</sup>. Furthermore, the PCI value per sample unit is calculated using the equation  $PCI = 100 - DV$ . The overall PCI value is determined from the average PCI value in the sample unit [12]. The PCI determination process as outlined in ASTM D5340 is highly dependent on the DV curve, which was originally developed in the United States. Since the runway characteristics and maintenance scenarios differ between countries, these curves can produce condition assessments that do not accurately reflect field conditions. Furthermore, the process is costly and time-intensive as it includes analyzing up to 16 types of damage.

Airport pavement damage begins as soon as pavement is subjected to aircraft traffic. In its early stages, damage manifests as longitudinal and transverse cracks, weathering, and raveling. Over time, further damage includes block cracking, potholes, and rutting. Eventually, advanced damage such as alligator cracks and settlements occurs [13]. The type of crack damage can also occur from the top to the bottom of the pavement surface. Factors that cause this damage include traffic loads, temperature, asphalt mixture characteristics, and construction factors. Top-to-bottom cracks typically start as longitudinal cracks, which are followed by additional cracks 0.3–1.0 m apart. Eventually, transverse cracks connect these longitudinal cracks, forming patterns similar to bottom-to-top cracks [14]. The type of runway pavement damage is influenced by the thickness, material quality, aircraft load, weather conditions, and maintenance scenarios applied, all of which inform evaluation of pavement conditions.

Evaluation of airport pavement condition often relies on a deterioration value (DV) method, which uses a relationship curve between damage density and DV. Maintenance strategies are influenced by airport size and current field conditions. Standard DV curves frequently produce assessments inconsistent with field observations. Studies in Korea address this issue by developing DV curves tailored to local maintenance characteristics. Common types of flexible pavement damage include alligator cracking, block cracking, joint reflection cracking, longitudinal and transverse

cracking, patching, and rutting. Based on dominant damage types, Korean authors create DV curves through panel discussions among pavement experts who assess field images of various damages. Statistical analysis of these assessments yields a DV-density curve, which is then validated against field data. This method leads to pavement condition values 4.6 points lower than the standard method, proving that expert perception significantly influences DV curve development and PCI calculation [15]. The study directly proves that expert perceptions influence the shape of the DV curve in determining the PCI value of airport pavement. Furthermore, the DV curve model determines the PCI value and greatly influences the airport pavement maintenance management scenario. However, the evaluation method proposed in the study considers all types of damage but does not consider the ideal sample unit size needed to achieve a low standard deviation in PCI values. Although identifying all damage types in PCI evaluations provides comprehensive data, it does not effectively address the cost and time constraints faced in the field today. The use of standard sample unit sizes often leads to PCI data distributions with high standard deviations, which can impact maintenance decision-making. Therefore, this study aims to propose a refined PCI evaluation method that focuses observations on the primary types of runway damage.

The management of airport pavement can generally be grouped into two major parts, namely (1) Network-Level and (2) Project-Level Management. At the network level, short- to medium-term budgeting needs analysis is carried out to determine which areas need to be followed up on at the project level. At the project level, decisions are made on the best maintenance scenario regarding cost where more detailed information is needed [16]. The application of network-level management to manage many airports is certainly a challenge. In addition to requiring large pavement condition investigation costs, the application also has the potential to produce inaccurate information due to less detailed data. At the network level, the process of predicting future conditions also contributes to greater decision-making errors. This can happen because the estimator only considers the main factors, such as aircraft traffic load. The pavement condition prediction model should follow airport pavement planning design development.

Airport pavement planning design has evolved from empirical to mechanistic-empirical methods. In the mechanistic-empirical method, environmental loads are also considered in addition to aircraft traffic load factors. This affects the paradigm of pavement condition values, which should not be limited to observations of damage due to loads and environmental factors. Environmental factors produce a fatigue model with a minimum tensile stress value. However, when combined with aircraft loads, it produces maximum tensile stress. The pavement condition value model is a function of pavement age and cumulative fatigue [17]. The pavement age variable is the primary predictor of PCI decline, as it comprises key technical factors such as asphalt aging, accumulated aircraft traffic loads, and environmental exposure to heat and rain. Various studies have developed PCI decline models based on different airport characteristics, but these models are not universally applicable across all countries. As a tropical country with two distinct seasons and high domestic air traffic, Indonesia exhibits a different PCI decline pattern compared to airports in four-season climates. Using an unsuitable model for PCI prediction can lead to inefficiencies in maintenance costs. To address the inefficiencies, this study aims to propose a PCI decline trend model tailored for airports in tropical climates.

Based on the review of several publications, pavement condition parameter is a crucial evaluation element in determining airport maintenance scenarios. However, airport PCI evaluation requires great effort, including time and cost, necessitating the development of a more efficient evaluation procedure. It is also necessary to adjust the DV curve model to suit conditions in Indonesia in reducing the potential errors in determining airport pavement conditions. To reduce the potential for large bias in the PCI value analysis, studying the area of the sample unit that produces better data distribution is crucial. Therefore, this study proposes an alternative PCI evaluation method that focuses on analyzing the primary types of damage using a grid-based layout of a specific size. The analysis also examines PCI decline levels using pavement age as a key predictor to support the development of maintenance scenarios.

This study has various stages, and Section 1 describes the background and objectives of the publication. Section 2 describes other studies relevant to the PCI survey method, pavement damage interpretation, and PCI deterioration prediction model. Furthermore, Section 3 describes the methods used, including the location, runway damage data collection techniques, panel rating method, development of deduct value model, and application of airport PCI evaluation method. Based on this methodology, the analysis and results are discussed in Section 4. The subsequent stage, including Section 5, presents the conclusions and further analysis that need to be carried out to complement the results.

## 2. Literature Review

### 2.1. Airport Pavement Planning

In airport flexible pavement planning, the failure criteria of vertical strain ( $\epsilon_v$ ) above the subgrade and horizontal strain ( $\epsilon_h$ ) below the asphalt mixture was used. Fatigue failure was calculated as the Cumulative Damage Factor (CDF) value [18]. The CDF value also predicted the remaining life of pavement [19]. Fatigue failure in airport pavements was characterized by the appearance of cracks from the bottom of the asphalt mixture and propagating to the surface [20]. Crack damage starting at the pavement surface and spreading downward generally occurred in the wheel path [14].

## 2.2. Airport Pavement Maintenance

Although designed for a 20-year lifespan, pavement conditions typically became unsuitable for use without rehabilitation by the 10th to 15th year [21]. Figure 1 showed the concept of airport pavement preservation, showing that timely maintenance preserved the functional age of pavement in good condition throughout the planned life. An analysis of pavement with a PCI value of 80 showed that postponing maintenance by a year potentially increased life cycle costs by up to 16% [22]. Despite widespread use, maintenance scenarios based on visual surveys of pavement conditions did not guarantee accurate condition predictions [23]. Airport pavement maintenance methods evolved from basic techniques to the incorporation of advanced information technology. Furthermore, a study utilizing 356 dataset from 26 airports in China employed data mining techniques to support maintenance decision-making by considering factors such as budget constraints, allowable delays, anticipated benefits, and safety parameters, resulting in a model with high predictive accuracy [24].

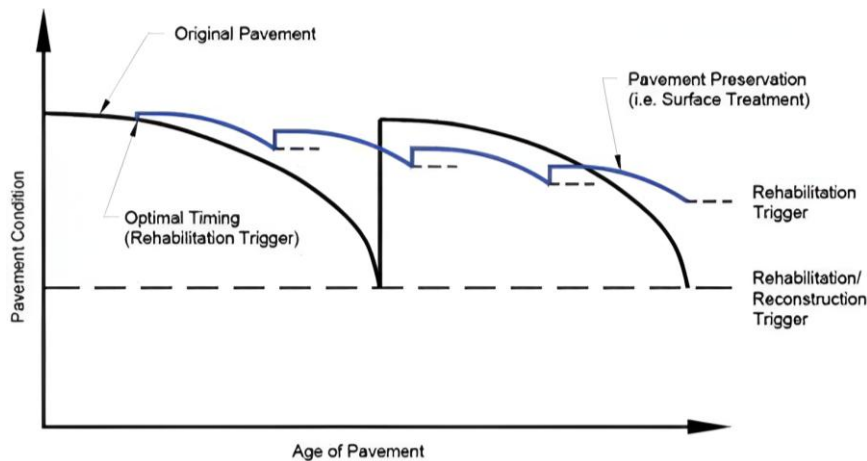


Figure 1. Pavement Preservation Concept [16]

## 2.3. Pavement Damage Detection

Airport PCI evaluation was preceded by collecting damage data on the runway, where the detection was generally carried out by visual observation in the field. This procedure had the disadvantage of being subjective, depending on the knowledge and experience of the field technical team in terms of runway pavement. Damage detection on runway pavement had also been widely studied by using the development of information technology. Crack photos were obtained through several methods, namely (1) visible light-based imaging from satellites, surfaces, or microscopes; (2) laser-based imaging for 3-dimensional analysis; (3) computer tomography (CT) for micro-crack analysis in laboratories; (4) radar imaging for crack depth measurements; (5) ultrasonic imaging for wave transformations; and (6) infrared imaging for crack depth assessment [25]. Crack pixels were detected using the adaptive threshold method, achieving accuracy, recall, and F values of 91.20%, 97.99%, and 94.12%, respectively [26].

Besides the high-resolution photos, drone photography in crack detection has also been studied using the U-Net architecture. The performance measures included F1, precision, recall, and Intersection over Union (IoU). The study object was the runway of Fitchburg Municipal Airport (FMA) in Massachusetts. The application of the U-Net architecture to image detection sourced from Crack500 obtained an IoU performance of 0.60. Based on this study, the authors stated that the U-Net architecture was promising in detecting cracks on the runway and could be followed up by using the results to calculate the PCI value [27].

In another publication, runway crack detection of 3,281 data samples showed that the YOLOv5 algorithm was superior to other traditional algorithms [28]. The rutting modeling used a machine learning (ML) method with four different algorithms, namely Support Vector Regression (SVR), Random Forest (RF), Artificial Neural Network (ANN), Gradient Boosting (GB), and multi-variable linear regression. The GB algorithm produced the best model performance with an  $R^2$  value = 0.92 in predicting rutting depth [29]. The method of pavement damage classification using a Convolutional Neural Network (CNN) model applied to 2,105 high-definition photos of various dominant damage types produced fairly reliable results. Furthermore, the true positive rate parameter expressed the reliability of the CNN model. The true positive rate values obtained were 75.8% for pothole damage, 84.1% for patch damage, 76.3% for markings, 79.4% for longitudinal cracks, and 83.1% for block crack damage [30].

In certain cases, pavement conditions could not be properly predicted using only damage photo processing. This was because two-dimensional photos described damage conditions with depth attributes, both cracks and rutting. To address this problem, the minimal patch selection algorithm could be used [31]. Another method that could be used was LiDAR in addition to using photos in damage detection. Tests showed that pavement damage detection using LiDAR could

speed up data acquisition process. On certain high-spec equipment, the LiDAR was able to detect small-width cracks on runways and potholes on highways [32].

Condition and IRI prediction models were analyzed from 8,275 photos containing PCI, IRI, and crack percentage information with a total data of 24,825. The study showed that the PCI value was highly correlated with the IRI value with an  $R^2$  value of 0.895 [33]. The use of the Automated Road Survey System in the survey of small airport pavement conditions in India was also carried out using the ASTM D5340 calculation procedure assisted by PAVER and Geographic Information System (GIS)-based software [34]. A PCI study using drones as a data collection method showed good prospects in damage detection. The PCI value of the photo processing results using the image processing method was 56.5 compared to 54.0 when conducted manually [35].

### 2.4. Prediction of Airport Pavement Conditions

The prediction of PCI values was studied by considering factors influencing the deterioration in PCI values. Table 1 presented several PCI reduction models that were analyzed in previous studies. Most of these models were developed with pavement age as the primary variable triggering PCI reduction, largely due to the ease of obtaining pavement age data from APMS reports at airports. Other factors, such as pavement type, climate, pavement thickness, and aircraft traffic, also influenced PCI reduction. However, accessing this information required greater effort.

**Table 1. Variables in PCI value prediction**

No.	Study (year)	PCI prediction variables
1	Suh et al. (2002) [36]	Age
2	Yuan & Mooney (2003) [37]	Age, pavement type, pavement function, construction and maintenance history, climate, base layer drainage conditions, and pavement thickness
3	Tarefder & Rahman (2016) [38]	Initial PCI
4	Camarena Campos & Flores Gonzales (2018) [39]	Age
5	Saleh et al. (2020) [40]	Age
6	Kwak et al. (2021) [41]	Age, slab thickness, air temperature
7	Di Mascio et al. (2021) [42]	Age, air temperature
8	Ashtiani (2021) [43]	Age
9	Ali et al. (2022) [44]	IRI

## 3. Methodology

### 3.1. Study Location

The study was conducted at 18 airports in Indonesia, spread across Sumatra, Java, and Kalimantan islands. Runway damage analysis was performed at these locations, representing 40 major airports in the country. In 2019, the total aircraft movements at the study airports amounted to 381,745, accounting for 34.0% of the national total of 1,123,042 movements. By 2023, these airports recorded 248,821 movements, representing 26.2% of the national total of 1,013,712 movements. The study locations and runway general information are presented in Figure 2 and Table 2, respectively.

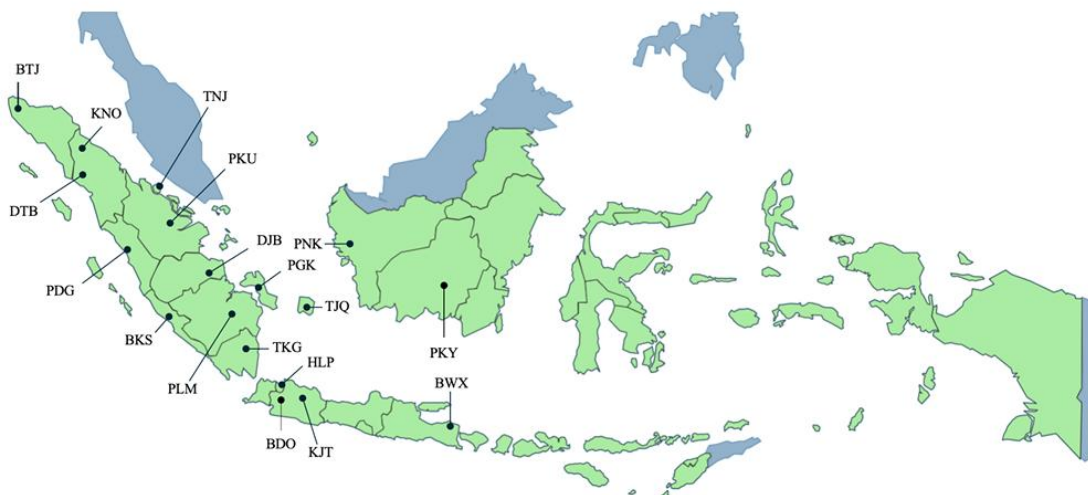


**Figure 2. Study Locations at 18 Airports in Indonesia**

**Table 2. General Information on Studied Airport Runways**

No.	Airport	Runway Size (m × m)	PCN	No.	Airport	Runway Size (m × m)	PCN
1	BTJ	45 × 3.000	88 F/C/W/T	10	TKG	45 × 2.770	63 F/C/X/T
2	KNO	60 × 3.750	71 F/B/W/T	11	PGK	45 × 2.250	65 F/B/W/T
3	DTB	45 × 2.650	40 F/C/X / T	12	TJQ	45 × 2.500	46 F/C/X/T
4	TNJ	45 × 2.500	61 F/C/X/T	13	HLP	45 × 3.000	89 F/C/X/T
5	PDG	45 × 3.000	89 F/C/X/T	14	BDO	45 × 2.250	50 F/C/X/T
6	PKU	45 × 2.600	66 F/B/X/T	15	KJT	60 × 3.000	89 F/C/X/T
7	BKS	45 × 2.250	51 F/C/X/T	16	PNK	45 × 2.600	51 F/D/X/T
8	DJB	45 × 2.602	65 F/B/X/T	17	PKY	45 × 2.500	48 F/C/W/T
9	PLM	45 × 3.000	80 F/C/X/T	18	BWX	45 × 2.450	56 F/C/X/T

**3.2. Study Flowchart**

This study was conducted in four stages, including literature review, survey design, data collection & field survey, as well as analysis and discussion. The literature review included mapping relevant studies related to airport pavement planning, management, condition evaluation methods, application of artificial condition networks, and PCI deterioration prediction models. The subsequent step was to conduct survey planning, including selecting a pavement expert panel and preparing a pavement condition value perception form. The next stage included collecting secondary data and conducting a field survey. The secondary data collected consisted of (1) the Annual Report on Airport Pavement Management System, (2) the Annual Report on Aircraft Traffic, and (3) the Airport Pavement Condition Report. Field surveys were conducted to evaluate the condition of runway pavement, with secondary data collected at 18 airports and field surveys at 3 airports. Based on the initial analysis of the dominant types, a condition perception survey was conducted with the expert panel. The expert panel evaluated damage types limited to those statistically identified as dominant. In the final stage, a deduct value curve model was developed based on the expert panel's perceptions. The resulting model was tested using PCI calculations, and the analysis results justified developing the PCI evaluation procedure (see Figure 3).

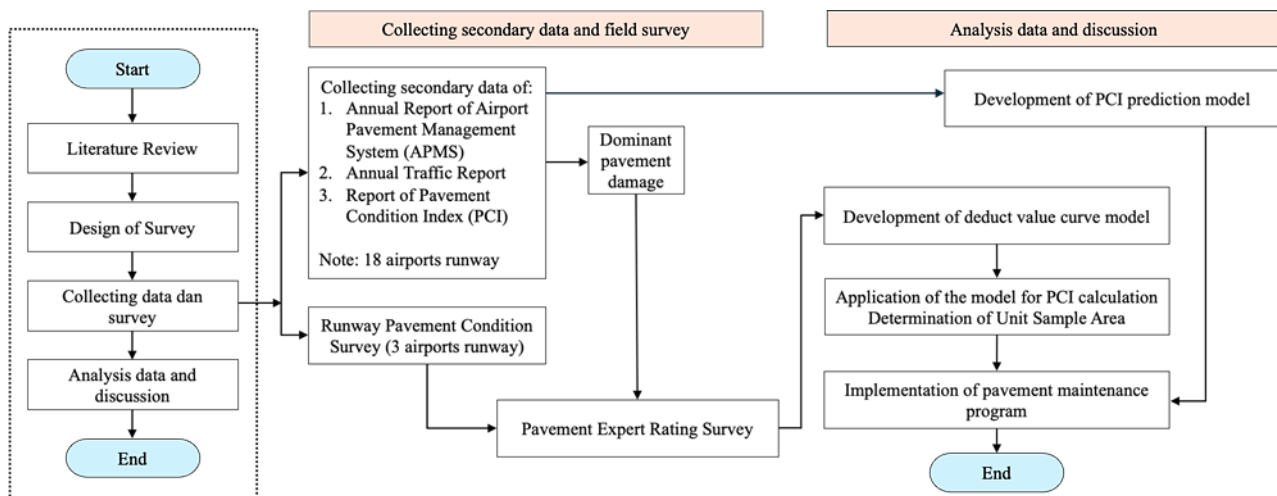


**Figure 3. Study Flowchart**

**3.3. Survey Method of Runway Pavement Condition**

The field pavement condition survey was conducted at three airports, including PKY, TJQ, and TKG. These airports had runway lengths of 2,500 m, 2,500 m, and 2,770 m, respectively. The selection of these three airports as field survey locations was based on the criterion of pavement age (>3 years). PKY, TJQ, and TKG airports had runway pavements aged 4.5 and 7 years, respectively. At that age, airport pavements in Indonesia had generally shown various types of damage. The selection of these three airports was expected to be fairly representative of other airports with pavement ages ranging from 1 to 10 years. In contrast to the general evaluation carried out by dividing the sample into a certain area (e.g., 450 m<sup>2</sup>), this study did not define a specific sample unit area. The survey was carried out by inspecting the runway using a vehicle and recording damage types, severity levels, extents, and locations. Damage locations were marked by determining coordinates based on damage geometry. Figure 4 described the survey method in the study. The runway was also assumed to lie on a plane with the X-axis representing the length and the Y-axis showing the width. The survey began at X = 0 and proceeded to the opposite runway end. The type of damage found on pavement (raveling/weathering, alligator cracking), severity levels (low, medium, high), area (in m<sup>2</sup>), and location coordinates were recorded.

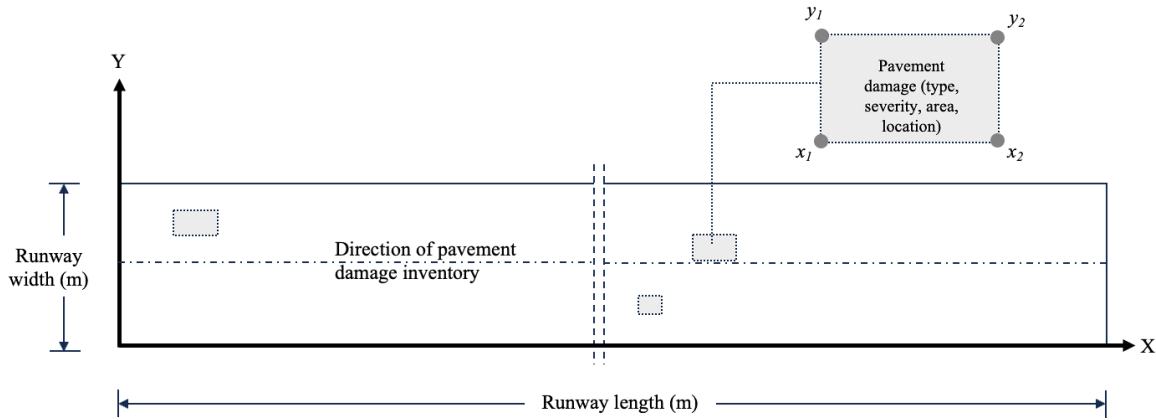


Figure 4. Survey Method of Runway Pavement Damage

3.4. PCI Calculation

PCI was calculated by subtracting the maximum pavement condition ( $C$ ) from the deduct value which depended on damage type ( $T_i$ ), severity ( $S_i$ ), and damage density ( $D_i$ ). Equation 1 was used to calculate the PCI while variables  $i, j$ , and  $p$  represented the amount, level, and number of damage types considered.  $F(t, d)$  served as an adjustment factor connected to the total deduct value ( $TDV$ ) ( $t$ ) and the number of deducts ( $d$ ).

$$PCI = C - \sum_{i=1}^p \sum_{j=1}^{m_i} a(T_i, S_j, D_{ij}) F(t, d) \tag{1}$$

The deduct value was calculated using the curve model generated from analysing the perception of damage conditions to the expert panel.

3.5. Development of the Deduct Value Curve Model

The deduct value curve, which reduces pavement condition value, was derived using the expert panel perception method. The flowchart of deriving the deduct value curve model was shown in Figure 5. The input data required in this analysis were historical information on airport pavement conditions and field data, including the damage type as well as level and documentation photos of pavement damage. The data showed that the damage type was evaluated according to the type and level of damage (low, medium, and high) and density within each sample unit. A single sample unit covered a 450 m<sup>2</sup> runway surface area. The next step was to conduct a statistical analysis to obtain a range of density values by dividing data into five classes. Density classification was also needed to obtain opportunities for both linear and non-linear models. In each density class, several examples of field photos were determined and further assessed for condition value (0-100). Furthermore, the deduct value was obtained by subtracting 100 from the condition rating value of the experts. At the end of the analysis, a curve model regression was carried out by determining the X-axis as the density and the Y-axis as the deduct value. This was performed for various types of dominant damage based on the damage level.

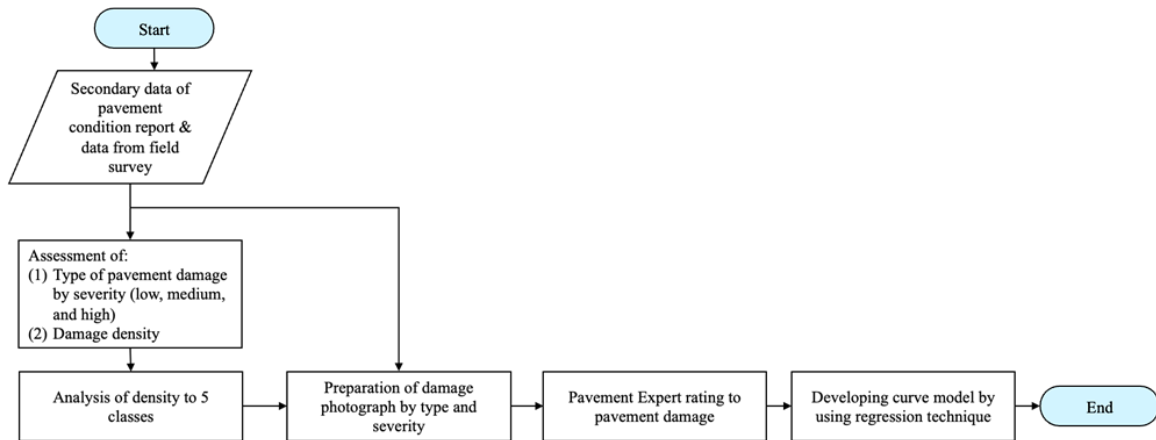


Figure 5. Flowchart of the Deduct Value Curve Model Development

Before conducting the regression, data filtering was performed using the Interquartile Range (IQR) method to obtain a robust model and minimize bias from the expert panel's perception. According to this method, the lower limit was determined as  $Q1 - 1.5 * IQR$  and the upper limit as  $Q3 + 1.5 * IQR$ , where  $IQR = Q3 - Q1$ .  $Q1$  and  $Q3$  represented the first and third quartiles of the data, respectively.

The deduct value curve model was analyzed through regression analysis with density on the X-axis and deduct value on the Y-axis. Linear, logarithmic, and power patterns were considered for modeling the relationship between deduct values and damage density.

$$DV = a + b.D \tag{2}$$

$$DV = a + b.Ln(D) \tag{3}$$

$$DV = a.DV^b \tag{4}$$

### 3.6. Determination of Sample Unit Area

The sample unit area was tested using the PCI analysis in transverse and longitudinal runway directions with various variations in area size. Figure 6 showed the assumptions of variations in the area and orientation of the sample unit. The left image showed the sample unit area in the transverse direction of the runway with dimensions ( $x_{tr} \times y_{tr}$ ). In the longitudinal direction of the runway, the sample unit was modeled with an area of ( $x_{lg} \times y_{lg}$ ). In the transverse direction, the sample unit dimensions of 5 m × 45 m (225 m<sup>2</sup>), 10 m × 45 m (450 m<sup>2</sup>), and 15 m × 45 m (675 m<sup>2</sup>) were tested. The same area variation was treated in the longitudinal direction but with different length and width configurations. The sample unit sizes tested in this direction included 25 m × 9 m (225 m<sup>2</sup>), 50 m × 9 m (450 m<sup>2</sup>), 75 m × 9 m (675 m<sup>2</sup>), 15 m × 15 m (225 m<sup>2</sup>), 30 m × 15 m (450 m<sup>2</sup>), and 45 m × 15 m (675 m<sup>2</sup>). Each sample unit size and orientation variation was applied to the PCI calculation at PKY, TJQ, as well as TKG airports, and the results were further analyzed. The optimal sample unit area was determined as the one with an average PCI value yielding the lowest standard deviation, below 10 (standard deviation <10).

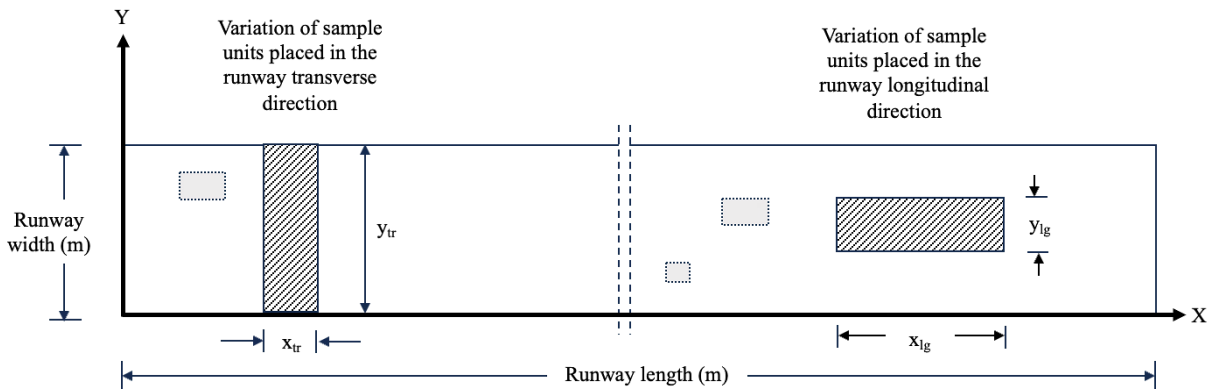


Figure 6. Variation of the Sample Unit Area and Orientation on the Runway

### 3.7. Development of PCI Prediction Model

The PCI deterioration model was developed using data from APMS database for the 18 study airports. The database contained the history of runway pavement construction and PCI values. Based on these data, the age of pavement at each airport location was analyzed which was defined as the time from the last overlay to the PCI evaluation date. Regression analysis was performed on the age and PCI value data for each review year to establish the PCI deterioration model. Observations from 2019–2023 were also included in the analysis where Figure 7 showed an illustration of determining pavement age and the corresponding PCI value in developing the PCI prediction model.

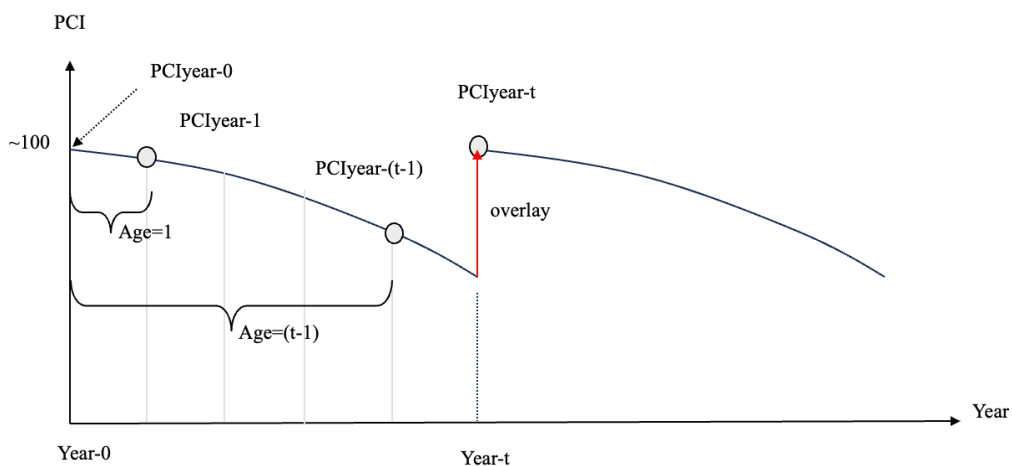


Figure 7. Determination of Pavement Age in the PCI Prediction Models Development

## 4. Results and Discussion

### 4.1. Dominant Types of Damage on the Runway

Based on the analysis of runway damage data at 18 airports in 2020, 5,994 damage locations were found. The dominant types of damage were raveling and weathering (25.84%), patching (18.09%), alligator cracking (13.17%), and rutting (9.66%). In 2021, the composition of the types of damage found in the field also showed that these four types still dominated. Figure 8 showed the dominant types of damage on the runway in 2020 and 2021 at the 18 airports.

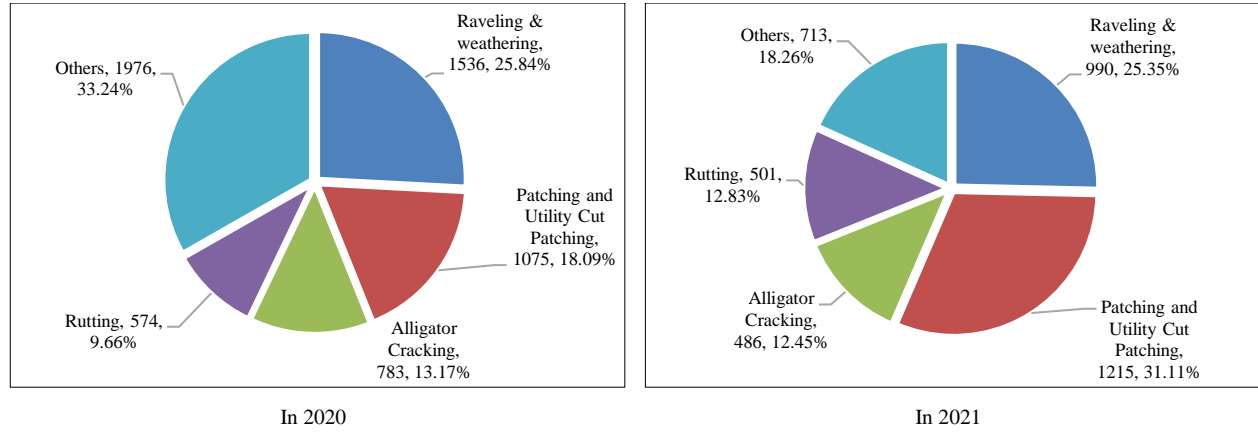


Figure 8. Types of Dominant Pavement Damage on the Runway

Raveling & weathering-type damage described the condition of the asphalt mixture exposed to the environment. High temperatures and rainfall contributed to weathering, leading to the release of aggregate grains. Alligator cracking, which was a type of fatigue damage, occurred in areas subjected to repeated aircraft loads. In these areas, the tensile strain beneath the asphalt surface exceeded permissible limits. Rutting, which was a form of permanent deformation, was developed in the aircraft wheel track areas due to repeated loading. In this condition, the asphalt mixture surpassed the elastic limit, preventing the pavement from returning to the original shape. Patching, which was classified as a type of damage, included replacing damaged pavement areas. This was considered a form of damage because the specifications of the patched areas often differed from and were generally inferior to the surrounding pavement.

Based on evaluation results, development of the deduct value curve focused on the dominant damage types, including raveling and weathering, patching, alligator cracking, and rutting. These four damage types were prioritized in assessing airport pavement conditions.

### 4.2. Damage Density Characteristics

Damage density was a parameter used to assess pavement conditions. Higher damage density corresponded to a lower pavement condition value. The damage density in each sample unit was calculated by dividing the damaged area by the total area of the sample unit. An analysis of raveling and weathering damage data at PKY, TJQ, and TKG airports produced a density classification summarized in Table 3. The highest observed density reached 70.29%, showing that damage in a sample unit area of 450 m<sup>2</sup> covered 316.3 m<sup>2</sup>.

Table 3. Damage Level, Density Class, and Field Condition Photos of Raveling & Weathering Damage

Density Class (%)	Damage level		
	Low	Medium	High
1 1.55 – 9.89			
2 9.89 – 15.89			



Another dominant type of damage was patching, a form of handling damage that occurred on airport pavements. Density classes could be grouped into five classes with a maximum damage density level reaching 13.96% of the sample unit area of 450 m<sup>2</sup>. Table 4 further showed examples of photo documentation of the damage divided according to density class and level of damage.

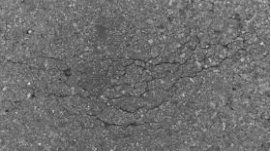
**Table 4. Level of Damage, Density Class, and Photos of Field Conditions on Patching Damage**

Density Class (%)	Damage level		
	Low	Medium	High
1 0.10 – 0.44			
2 0.44 – 1.32			
3 1.32 – 4.66			
4 4.66 – 7.11			
5 7.11 – 13.96			

The alligator cracking damage type exhibited varying conditions, with density values ranging from 0.09% to 25.38%. This type of damage represented a form of pavement fatigue failure caused by the repeated loading of aircraft wheels. It originated at the bottom of the asphalt mixture and propagated to the surface. Table 5 presented examples of field photos showing alligator cracking conditions at different density levels and degrees of severity.

Table 6 shows the runway pavement condition affected by rutting damage. This form of damage occurred when pavement lost elasticity, typically along the aircraft wheel path. The density values were categorized into five classes, namely 0.65%-3.73%, 3.73%-5.38%, 5.38%-7.33%, 7.33%-9.17%, and 9.17%-19.18%.

**Table 5. Damage Level, Density Class, and Field Condition Photos of Alligator Cracking Damage**

Density Class (%)	Damage level		
	Low	Medium	High
1 0.09 – 1.32			
2 1.32 – 2.58			
3 2.58 – 4.45			
4 4.45 – 7.92			
5 7.92 – 25.38			

**Table 6. Level of Damage, Density Class, and Photos of Field Conditions for Rutting Damage**

Density Class (%)	Damage Level		
	Low	Medium	High
1 0.65 – 3.73			
2 3.73 – 5.38			
3 5.38 – 7.33			
4 7.33 – 9.17			
5 9.17 – 19.18			

The described damage characteristics were incorporated into a panel discussion with pavement experts. During the discussion, the experts provided assessments of pavement condition values (0–100) for pavements exhibiting raveling & weathering, patching, alligator cracking, and rutting damage. These assessments were subsequently analyzed to develop a deduct value curve model.

#### 4.3. Development of the Deduct Value Curve Model

Following the previously outlined methodology, the deduct value curve model was developed using the expert panel perception method. Panel members were selected based on the professional expertise in pavement planning and maintenance. The expert panel comprised 40 individuals with the following composition namely airport operators (60.0%), representatives from the Ministry of Public Works and Public Housing (15.0%), consultants (10.0%), academics (7.5%), officials from the Ministry of Transportation (5.0%), and airport contractors (2.5%). Figure 9 further showed the composition of the expert panel included in evaluating airport pavement conditions.

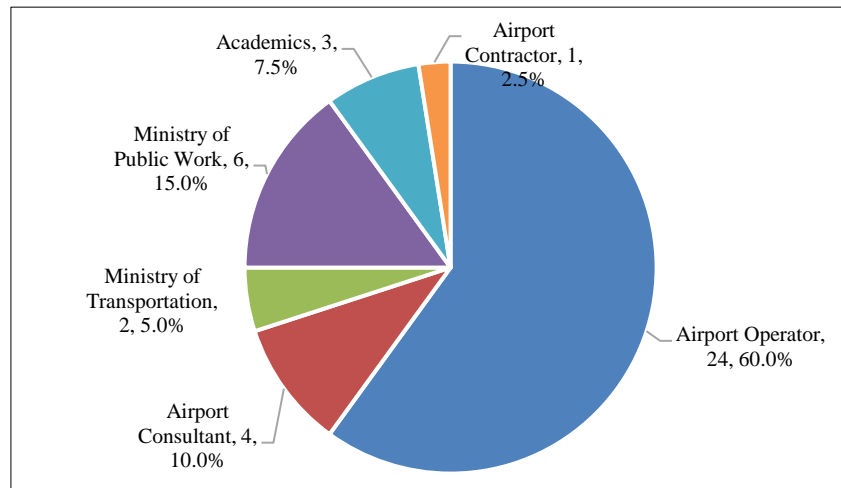


Figure 9. Expert Panel Profile

The expert panel's perception of pavement condition value was based on conditions discussed during the session. Based on the expert panel category, there were six types of expert panels with different professional backgrounds. This variation introduced the potential for bias in the perception of pavement conditions. To minimize bias, data filtering was conducted to eliminate outliers, following the method previously explained. In this study, condition value was assumed to be the PCI. The deduct value was calculated using the equation:  $\text{Deduct Value (DV)} = 100 - \text{PCI}$ . By using various combinations of density values (D), pairs of DV and D values were obtained, which were then developed into a mathematical model to describe the relationship between the two. Table 7 provided a summary of the deduct value curve model for various types of damage, levels of damage, and the corresponding linear (1), logarithmic (2), and power (3) models.

The deduct value curve model for raveling and weathering damage at various severity levels was developed using the power model, as it further showed the lowest RMSE performance. Additionally, the RMSE values for low, medium, and high damage levels were 0.87, 1.39, and 0.94, respectively. For patching-type damage, the logarithmic model was selected for low and medium severity levels, while the power model was chosen for high severity. The  $R^2$  values of selected models were 0.88, 0.88, and 0.75 for low, medium, and high severity levels, respectively.

For alligator cracking, the logarithmic model was selected for low, medium, and high damage levels, as it produced the highest  $R^2$  values of 0.89, 0.92 and 0.88. For rutting-type damage, the logarithmic model was selected across all severity levels, as it consistently provided the highest  $R^2$  values compared to other models. For instance, at low damage levels, the power model achieved an  $R^2$  of 0.86, outperforming the power model ( $R^2 = 0.83$ ) and the linear model ( $R^2 = 0.74$ ).

In addition to the  $R^2$  and RMSE, model accuracy was also evaluated based on the confidence interval with a narrower confidence interval showing greater precision in the estimates. Furthermore, practicality was considered when plotting the curve to ensure there were no intersections between damage levels, as such intersections could lead to inconsistencies in the resulting deduct values.

Based on the analysis of damage density characteristics, the study found that each damage type had a different density range where no sample unit exhibited a density of 100%. The highest density values for the various types of damage were 70.29%, 13.96%, 25.38%, and 19.18% for raveling & weathering, patching, alligator cracking, and rutting damage, respectively. The curve model proposed in this study considered both the  $R^2$  performance and flexibility.

Furthermore, flexibility refers to the model's ability to accommodate damage densities up to 100%. This was done to prevent the curves from intersecting between those for low, medium, and high levels of damage. Figure 10 showed the results of the deduct value curve development for the four most common damage types at the study locations.

**Table 7. Results of the Deduct Value Curve Model Development**

No	Type of Damage	Level of Damage	Option	Curve Model	R <sup>2</sup>	RMSE	Confidence Interval (95%)
1	Raveling & Weathering	Low	1	$DV_{RW-L} = 0.2571 * D + 7.3428$	0.84	2.07	[13.84 – 15.04]
			2	$DV_{RW-L} = 5.9778 * \ln(D) - 3.6306$	0.89	1.38	[13.82 – 15.06]
			3*	$DV_{RW-L} = 3.0601 * D^{0.4858}$	0.88	0.87	[13.67 – 15.00]
		Medium	1	$DV_{RW-M} = 0.3871 * D + 20.49$	0.87	3.95	[38.43 – 40.94]
			2	$DV_{RW-M} = 16.6030 * \ln(D) - 22.302$	0.92	2.36	[38.40 – 40.98]
			3*	$DV_{RW-M} = 6.3462 * D^{0.4788}$	0.90	1.39	[38.18 – 40.91]
		High	1	$DV_{RW-H} = 0.3732 * D + 48.963$	0.58	6.03	[59.69 – 61.47]
			2	$DV_{RW-H} = 10.06 * \ln(D) + 28.584$	0.73	2.51	[59.58 – 61.58]
			3*	$DV_{RW-H} = 32.217 * D^{0.1932}$	0.71	1.05	[59.13 – 61.34]
2	Patching	Low	1	$DV_{PT-L} = 1.053 * D + 3.3541$	0.90	1.48	[7.65 – 8.75]
			2*	$DV_{PT-L} = 3.1085 * \ln(D) + 5.6304$	0.88	1.67	[7.65 – 8.75]
			3	$DV_{PT-L} = 4.5747 * D^{0.4699}$	0.92	0.94	[7.57 – 8.70]
		Medium	1	$DV_{PT-M} = 1.6475 * D + 9.9364$	0.90	2.20	[17.19 – 18.76]
			2*	$DV_{PT-M} = 7.091 * \ln(D) + 9.5797$	0.88	2.14	[17.45 – 19.10]
			3	$DV_{PT-M} = 10.344 * D^{0.4012}$	0.91	0.97	[17.24 – 18.83]
		High	1	$DV_{PT-H} = 2.9686 * D + 15.362$	0.86	3.12	[21.73 – 23.71]
			2	$DV_{PT-H} = 4.74 * \ln(D) + 22.543$	0.71	2.87	[21.83 – 23.62]
			3*	$DV_{PT-H} = 21.304 * D^{0.1974}$	0.75	0.94	[21.57 – 23.20]
3	Alligator Cracking	Low	1	$DV_{AC-L} = 1.5468 * D + 25.271$	0.76	5.11	[34.04 – 36.60]
			2*	$DV_{AC-L} = 8.806 * \ln(D) + 23.592$	0.89	3.72	[33.94 – 36.70]
			3	$DV_{AC-L} = 22.812 * D^{0.2851}$	0.87	1.67	[33.55 – 36.57]
		Medium	1	$DV_{AC-M} = 1.3496 * D + 36.004$	0.68	6.19	[43.41 – 45.91]
			2*	$DV_{AC-M} = 8.7259 * \ln(D) + 33.867$	0.92	11.27	[32.90 – 35.80]
			3	$DV_{AC-M} = 33.274 * D^{0.2111}$	0.88	10.29	[43.00 – 46.09]
		High	1	$DV_{AC-H} = 2.0161 * D + 41.359$	0.86	5.48	[52.30 – 56.10]
			2*	$DV_{AC-H} = 11.254 * \ln(D) + 40.945$	0.88	5.85	[52.27 – 56.13]
			3	$DV_{AC-H} = 40.947 * D^{0.2073}$	0.91	1.46	[52.09 – 55.92]
4	Rutting	Low	1	$DV_{RT-L} = 1.2623 * D + 16.099$	0.74	1.92	[23.11 – 24.00]
			2*	$DV_{RT-L} = 6.9434 * \ln(D) + 12.018$	0.86	0.91	[23.08 – 24.03]
			3	$DV_{RT-L} = 13.441 * D^{0.3283}$	0.83	0.37	[23.00 – 24.01]
		Medium	1	$DV_{RT-M} = 2.1787 * D + 23.436$	0.71	12.17	[21.57 – 22.33]
			2*	$DV_{RT-M} = 10.257 * \ln(D) + 19.103$	0.88	1.25	[21.29 – 22.28]
			3	$DV_{RT-M} = 20.399 * D^{0.3409}$	0.83	0.37	[21.16 – 22.14]
		High	1	$DV_{RT-H} = 1.8639 * D + 37.91$	0.72	2.83	[46.45 – 47.67]
			2*	$DV_{RT-H} = 10.433 * \ln(D) + 31.625$	0.84	1.15	[46.40 – 47.72]
			3	$DV_{RT-H} = 33.445 * D^{0.2263}$	0.82	0.33	[46.33 – 47.69]

\* Selected Model.

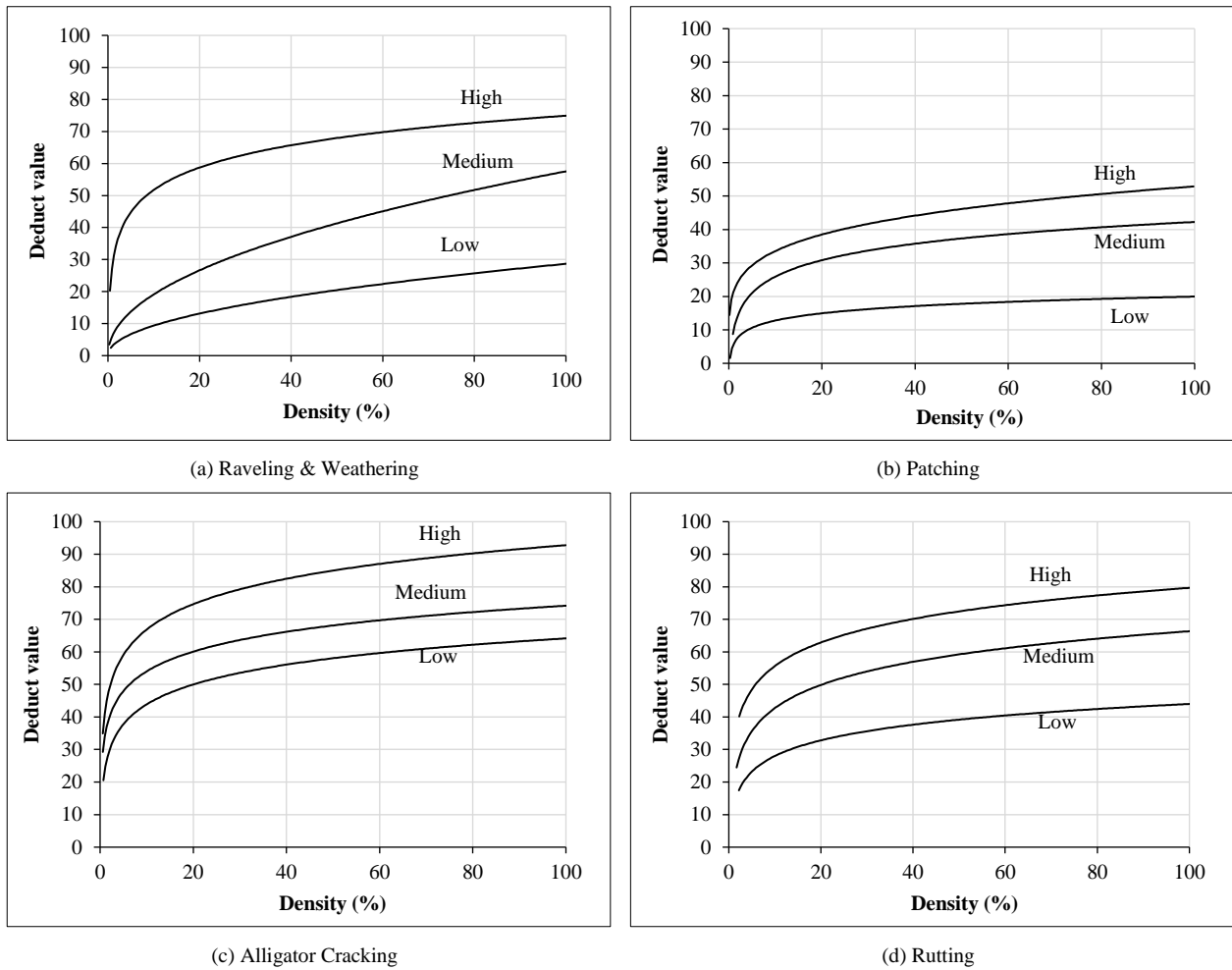


Figure 10. Curve Model of the Relationship between Density and Deduct Value

In addition to the deduct value curve model, this study also developed a corrected deduct value (CDV) curve model. This curve was necessary to adjust for sample units with more than one type of damage. A relationship curve between the TDV and CDV was proposed using the same method as shown in Figure 11. The curve's q value showed the number of damage types in a sample unit with a DV value > 5. For example, at q = 2, it showed that two damage types were found in the sample unit with a DV value > 5. The curves for q = 3 and q = 4 intersect at a TDV value of approximately 50 while the q = 4 and q = 5 curves intersect at a TDV value of around 120. The relationship curve between TDV and CDV was unique because it could account for sample unit conditions with TDV values as high as 260. This contrasted with a similar curve based on ASTM D5340 which accommodated a maximum TDV value of 180.

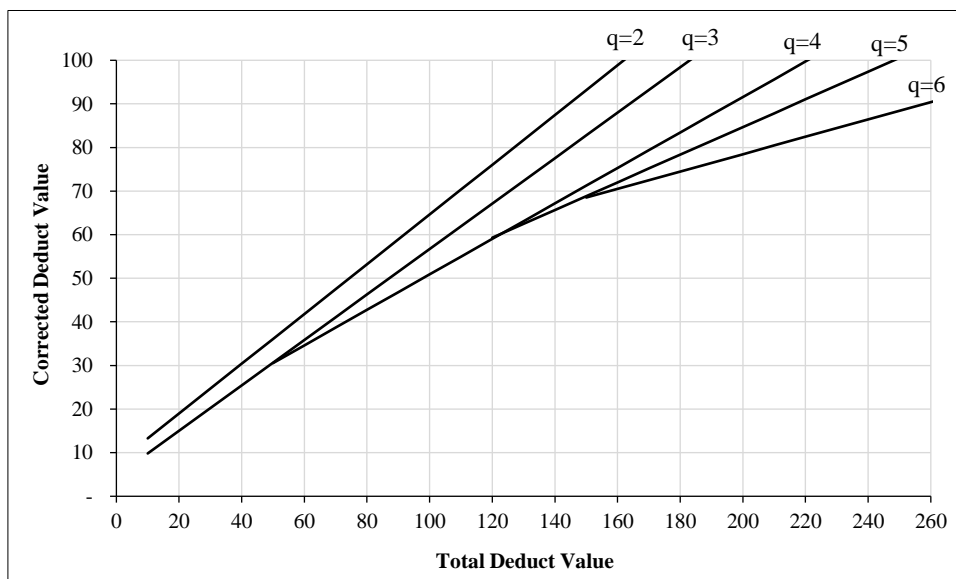


Figure 11. CDV Curve Model

$$q:2, CDV = 0,5704.TDV + 7,5768, R^2 = 0,9771 \tag{5}$$

$$q:3, CDV = 0,55214.TDV + 4,6126, R^2 = 0,917 \tag{6}$$

$$q:4, CDV = 0,4069.TDV + 10,199, R^2 = 0,9554 \tag{7}$$

$$q:5, CDV = 0,3173.TDV + 21,233, R^2 = 0,8919 \tag{8}$$

$$q:6, CDV = 0,1988.TDV + 38,706, R^2 = 0,8359 \tag{9}$$

A previous study by Cho et al. [15] modified the deduct value curve for six dominant types of pavement damage found in Korea namely alligator cracking, block cracking, joint reflection cracking, longitudinal and transverse cracking, patching, and rutting. After developing the deduct value curve model, PCI was calculated by replacing the ASTM D5340 standard curve with the modified curve for these six damage types, while other damage types remained unchanged in the PCI evaluation.

This study differs from the Korean publications in several aspects. Rather than considering six damage types, this study focused on PCI evaluation based on four main types of damage namely ravelling/weathering, patching, alligator cracking, and rutting. Another key difference was in the assumption regarding the sample unit area. In this study, variations in sample unit size were analyzed to determine the optimal size by evaluating the standard deviation of the resulting PCI data distribution.

#### 4.4. Application of Deduct Value Curve in PCI Evaluation

The deduct value curve model generated from the expert panel's perception was tested and applied to the PCI value evaluation at PKY, TJQ, and TKG airports. In this trial, damage data distributed across the runway was further analyzed. Therefore, it was possible to modify the area to 225 m<sup>2</sup>, 450 m<sup>2</sup>, and 675 m<sup>2</sup>. The sample unit area of 450 m<sup>2</sup> was the standard applied when referring to ASTM D5340. The purpose of varying the area was to assess the accuracy of the PCI value based on the standard deviation. The objective of the analysis was to determine the ideal area that would yield the smallest possible standard deviation. Table 8 shows the summary of the PCI analysis at the three airports.

**Table 8. PCI Value Evaluation on the Runway Transverse Direction Sample Unit**

PKY Airport			
Sample size	5×45	10×45	15×45
N	500	250	167
PCI <sub>average</sub>	52.54	51.72	65.73
Std.Dev	18.76	19.05	29.49
TJQ Airport			
Sample size	5×45	10×45	15×45
N	500	250	167
PCI <sub>average</sub>	50.64	50.02	47.55
Std.Dev	10.70	12.15	14.90
TKG Airport			
Sample size	5×45	10×45	15×45
N	556	278	185
PCI <sub>average</sub>	48.54	48.22	62.71
Std.Dev	10.99	11.89	24.93

The PCI values shown in Table 8 are the average PCI against the number of existing samples (N). Based on the results, it was observed that smaller sample unit sizes resulted in smaller standard deviations. For a sample unit size of 225 m<sup>2</sup>, the standard deviations obtained were 18.76, 10.70, and 10.99 for PKY, TJQ, and TKG airports, respectively. In contrast, at the largest sample unit size (675 m<sup>2</sup>), the standard deviation values at the three airports were 29.49, 14.90, and 24.93, respectively. As the sample unit size increased, the average PCI values became more dispersed from the mean.

The analysis of the runway longitudinal direction also showed a similar trend to that of the runway transverse direction, where smaller sample sizes produced lower standard deviations. However, in general, for the same area, the standard deviation of the sample unit placed in the runway longitudinal direction had a larger value. For example,

at PKY airport, a sample unit of dimensions (25×9) m<sup>2</sup> in the transverse direction had a standard deviation of 26.85, which was higher than the 18.76 standard deviation in the sample with dimensions (5×45) m<sup>2</sup> in the longitudinal direction. Table 9 summarizes the PCI value evaluation when the sample unit was placed in the runway longitudinal direction.

**Table 9. Evaluation of PCI Values on Runway Longitudinal Direction Sample Units**

PKY Airport						
Sample size (m x m)	25×9	50×9	75×9	15×15	30×15	45×15
N	500	250	167	500	250	167
PCI <sub>average</sub>	70.61	68.40	65.18	70.49	68.09	47.11
Std.Dev	26.85	27.74	29.19	27.64	29.09	19.33
TJQ Airport						
Sample size (m x m)	25×9	50×9	75×9	15×15	30×15	45×15
N	500	250	167	500	250	167
PCI <sub>average</sub>	73.48	72.36	71.28	69.22	66.72	49.24
Std.Dev	24.55	24.57	25.23	26.42	27.96	29.27
TKG Airport						
Sample size (m x m)	25×9	50×9	75×9	15×15	30×15	45×15
N	556	278	185	556	278	185
PCI <sub>average</sub>	69.49	67.20	64.92	64.85	62.85	45.82
Std.Dev	22.68	23.87	24.25	22.40	22.96	13.02

Based on the calculation results, the smallest sample size (225 m<sup>2</sup>) was found not to produce the expected standard deviation value (<10). A high standard deviation led to biased decision-making because with a high standard deviation, there was a possibility of a shift in pavement condition criteria. Consequently, pavement condition could have been addressed too late or even earlier than necessary, which would impact the overall maintenance life cycle costs. After going through a trial process with various sizes, a sample size was identified that allowed for an accurate PCI evaluation with a standard deviation value < 10. This was achieved with a sample unit dimension of 3 m × 5 m (15 m<sup>2</sup>). Figure 12 showed the layout concept and dimensions of the sample unit used in the PCI evaluation at airport. Applying sample unit dimensions of these sizes led to an average PCI value with a low standard deviation. Trials conducted at PKY, TJQ, and TKG airports yielded PCI values with standard deviations of 9.43, 6.14, and 8.09, respectively (see Table 10).

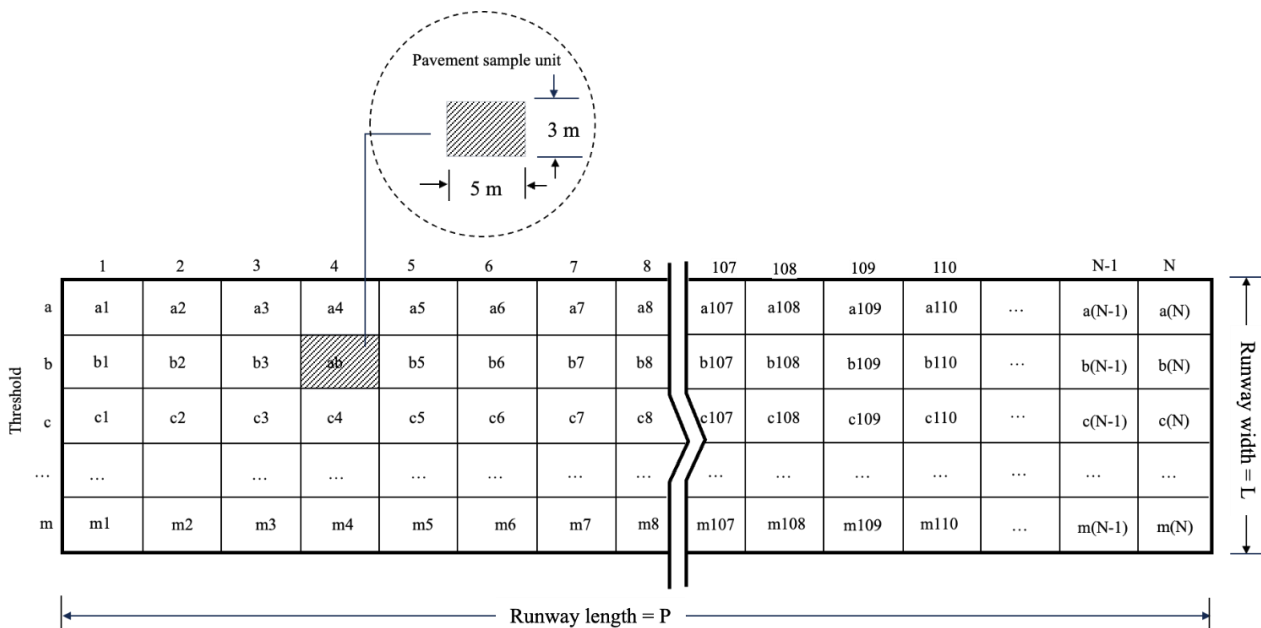


**Figure 12. Concept of the proposed PCI evaluation layout**

**Table 10. Statistical Performance of PCI Evaluation with Sample Unit Layout (3 × 5) m<sup>2</sup>**

	Airport		
	PKY	TJQ	TKG
N	7500	7500	8340
PCI <sub>average</sub>	78.14	80.75	76.83
Std. Dev	9.43	6.14	8.09

Various publications showed that combining the deduct value curve from this study with the proposed sample unit size resulted in PCI evaluations with low standard deviation values (ranging from 6.14 to 9.43). This was significantly lower compared to other sample unit sizes. For instance, in the transverse direction of the runway, a sample unit size of 450 m<sup>2</sup> produced standard deviations of 19.05, 12.15, and 11.89 at PKY, TJQ, and TKG airports, respectively (see Table 8).

Based on the distribution data of damage types as shown in Figure 8, the PCI evaluation method focusing on the four dominant damage types had the potential to reduce field survey time by up to 27.30%. Consequently, this proposed method effectively reduced both survey time and costs while maintaining the accuracy of PCI values.

**4.5. PCI Deterioration Model**

Based on the proposed method, airport PCI deterioration curve was estimated as shown in Figure 13. The deterioration curve was relatively flat, decreasing by 3.23 points per year. The PCI value decrease was similar to the study conducted by previous publication [42] with a decrease per year of 3 to 4 points. This flat deterioration was attributed to the runway pavement condition, which was consistently well-maintained. Additionally, the airport PCI evaluation was conducted across the entire pavement surface. In the aircraft wheel path area which extends from the runway centerline to the right and left within the lateral wander area, the PCI value was found to be 23.8% to 49.7% lower [45]. The PCI deterioration model was quite reliable ( $R^2 = 0.731$ ) when applied to pavements aged between 0-10 years, considering the distribution of airport sample data in Indonesia where runways had generally undergone overlays within the past 10 years. It was predicted that the curve would be steeper for pavements older than 10 years as the asphalt mixture would begin to age, weakening the aggregate binding power. Equation 6 showed the mathematical equation of the PCI deterioration curve.

$$PCI = 100 - 1.298.Age - 0.0207.Age^2, R^2 = 0.731 \tag{10}$$

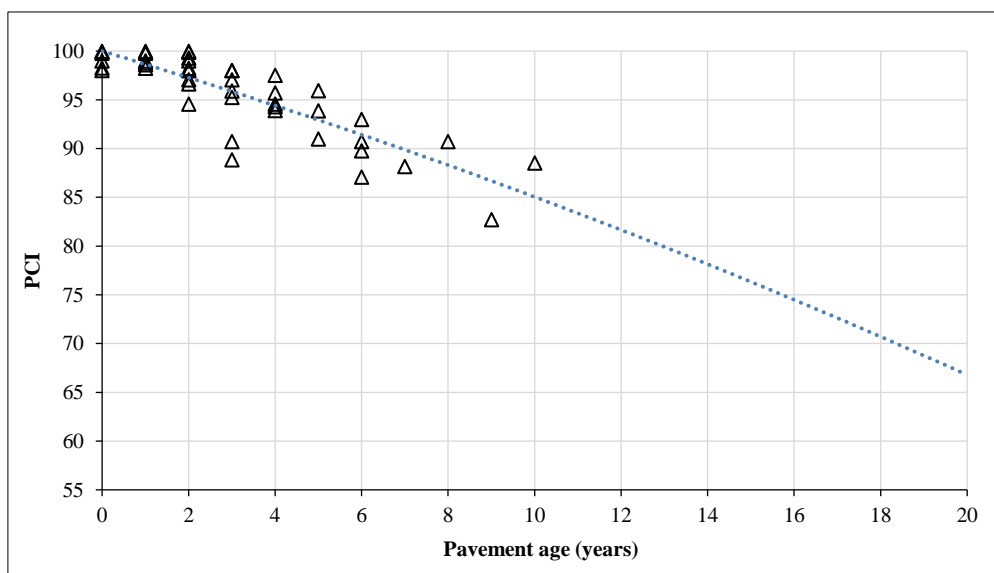


**Figure 13. PCI Prediction Curve as a Function of Pavement Age**

The PCI prediction curve could be considered for runway pavement maintenance scenarios. However, this curve could be supplemented with further studies, particularly for runways that were not well-maintained or were poorly maintained. In such conditions, PCI deterioration was predicted to occur at a faster rate.

The reduction in PCI value as a function of pavement age could be developed more comprehensively by incorporating variables such as load repetition, pavement structure, and air temperature. These three variables, along with pavement age, were expected to produce a more realistic model that could be applied more broadly to various airport locations.

## 5. Conclusions

In conclusion, this study successfully obtained a deduct value curve model to modify the existing deduct value curve. The model was considered more appropriate for application in Indonesia as it was derived from the perceptions of pavement experts included in airport planning in the country. By evaluating the sample unit's area, it was determined that both the area and orientation of the sample unit affected the final average PCI value at airports studied. The following conclusions were drawn from this study.

- The most common types of damage found at the study site were ravelling & weathering, patching, alligator cracking, and rutting. These four types were used as predictors of PCI values, producing good PCI predictions. It also saves time and reduces the cost of field investigations when compared to the ASTM D5340 procedure, which considers up to 16 types of pavement damage.
- The deduct value curve model for the damage types ravelling & weathering, patching, alligator cracking, and rutting was successfully developed with good performance. The distribution of expert panel perception data resulted in a model with a high  $R^2$  value for both linear, logarithmic, and power regression models.
- PCI evaluation of airport runway with a standard sample unit area of 450 m<sup>2</sup> led to a PCI standard deviation value of > 10 at the studied airport. At a sample unit area of 225 m<sup>2</sup>, a better standard deviation value was obtained, but it remained relatively high (> 10).
- The concept with a sample unit area of 15 m<sup>2</sup> (3 m × 5 m) proved to provide good statistical performance, with standard deviation values of 6.14 (TJQ), 8.09 (TKG), and 9.43 (PKY). The low standard deviation showed that the distribution of PCI data was close to the average value. Therefore, runway maintenance scheme decision-making could be better planned.
- The PCI model predicted as a function of pavement age led to an estimated decline of 3.23 per year across the 18 airports studied.
- The PCI evaluation method, which focused on four dominant types of damage (raveling/weathering, patching, alligator cracking, and rutting), had the potential to reduce field investigation time and costs by up to 27.30% based on the assumed distribution of damage types at the study locations.

Aside from the results achieved, this study needs further improvement, particularly by implementing artificial intelligence technology in evaluating PCI values. This technology was expected to reduce subjectivity in damage classification, save time and costs, increase accuracy, and ensure sustainable runway pavement management.

## 6. Declarations

### 6.1. Author Contributions

Conceptualization, A.W., B.S.S., A.S., and R.B.F.; methodology, A.W., B.S.S., and A.S.; formal analysis, A.W., B.S.S., and A.S.; investigation, A.W. and R.B.F.; data curation, A.W. and R.B.F.; writing—original draft preparation, A.W. and R.B.F.; writing—review and editing, A.W., B.S.S., and A.S.; supervision, A.W., A.S., and B.S.S.; funding acquisition, A.W. and B.S.S. All authors read and agreed to the published version of the manuscript.

### 6.2. Data Availability Statement

Data presented in this study are available on request from the corresponding author.

### 6.3. Funding and Acknowledgements

The authors are grateful to Angkasa Pura Indonesia for supporting data, as well as to Institut Teknologi Bandung for approving the funds used to effectively complete the study. All the contributions are acknowledged.

### 6.4. Conflicts of Interest

The authors declare no conflict of interest.

## 7. References

- [1] Chen, X., Xuan, C., & Qiu, R. (2021). Understanding spatial spillover effects of airports on economic development: New evidence from China's hub airports. *Transportation Research Part A: Policy and Practice*, 143, 48–60. doi:10.1016/j.tra.2020.11.013.
- [2] Mao, X., & Chen, X. (2023). Does airport construction narrow regional economic disparities in China? *Journal of Air Transport Management*, 108. doi:10.1016/j.jairtraman.2023.102362.
- [3] Uchida, K., Kato, H., Murakami, J., & Takeuchi, W. (2024). Does new airport investment promote urban economic development?: Global evidence from nighttime light data. *Transportation Research Part A: Policy and Practice*, 180. doi:10.1016/j.tra.2023.103948.

- [4] Zhu, X., Wu, Y., Yang, Y., Pang, Y., Ling, H., & Zhang, D. (2024). Real-time risk assessment of aircraft landing based on finite element-virtual prototype-machine learning co-simulation on wet runways. *International Journal of Transportation Science and Technology*, 13, 77–90. doi:10.1016/j.ijst.2023.11.007.
- [5] Ling, J., Yang, F., Zhang, J., Li, P., Uddin, M. I., & Cao, T. (2023). Water-film depth assessment for pavements of roads and airport runways: A review. *Construction and Building Materials*, 392. doi:10.1016/j.conbuildmat.2023.132054.
- [6] Miah, M. T., Oh, E., Chai, G., & Bell, P. (2020). An overview of the airport pavement management systems (APMS). *International Journal of Pavement Research and Technology*, 13(6), 581–590. doi:10.1007/s42947-020-6011-8.
- [7] Di Graziano, A., Ragusa, E., Marchetta, V., & Palumbo, A. (2021). Analysis of an Airport Pavement Management System during the Implementation Phase. *KSCE Journal of Civil Engineering*, 25(4), 1424–1432. doi:10.1007/s12205-021-1884-x.
- [8] Alabi, B. N. T., Saeed, T. U., Amekudzi-Kennedy, A., Keller, J., & Labi, S. (2021). Evaluation criteria to support cleaner construction and repair of airport runways: A review of the state of practice and recommendations for future practice. *Journal of Cleaner Production*, 312. doi:10.1016/j.jclepro.2021.127776.
- [9] Wesolowski, M., & Iwanowski, P. (2020). Evaluation of asphalt concrete airport pavement conditions based on the Airfield Pavement Condition Index (APCI) in scope of flight safety. *Aerospace*, 7(6), 78. doi:10.3390/AEROSPACE7060078.
- [10] Santos, B., Almeida, P. G., Feitosa, I., & Lima, D. (2020). Validation of an indirect data collection method to assess airport pavement condition. *Case Studies in Construction Materials*, 13, e00419. doi:10.1016/j.cscm.2020.e00419.
- [11] Pietersen, R. A., Beauregard, M. S., & Einstein, H. H. (2022). Automated method for airfield pavement condition index evaluations. *Automation in Construction*, 141, 141. doi:10.1016/j.autcon.2022.104408.
- [12] ASTM D5340-20. (2023). Standard Test Method for Airport Pavement Condition Index Surveys. ASTM International, Pennsylvania, United States. doi:10.1520/D5340-20.
- [13] Li, Y., Zou, Z., Zhang, J., & He, Y. (2023). Study on the evolution of airport asphalt pavement integrated distress based on association rule mining. *Construction and Building Materials*, 369, 369. doi:10.1016/j.conbuildmat.2023.130565.
- [14] Canestrari, F., & Ingrassia, L. P. (2020). A review of top-down cracking in asphalt pavements: Causes, models, experimental tools and future challenges. *Journal of Traffic and Transportation Engineering*, 7(5), 541–572. doi:10.1016/j.jtte.2020.08.002.
- [15] Cho, N. H., Kwon, H. J., Suh, Y. C., & Kim, J. (2022). Development of Korea Airport Pavement Condition Index for Panel Rating. *Applied Sciences (Switzerland)*, 12(16), 8320. doi:10.3390/app12168320.
- [16] AC 150/5380-7B. (2014). Airport Pavement Management Program (PMP). Federal Aviation Administration, U.S. Department of Transportation, Washington, United States.
- [17] Park, H. W., Kim, J. M., Lee, J. H., Lee, D. S., & Jeong, J. H. (2023). Pavement Condition Index Model for Mechanistic–Empirical Design of Airport Concrete Pavements Considering Environmental Effects. *Buildings*, 13(10), 2512. doi:10.3390/buildings13102512.
- [18] AC 150/5320-6G. (2009). Airport Pavement Design and Evaluation. Federal Aviation Administration, U.S. Department of Transportation, Washington, United States.
- [19] Wei, B., & Guo, C. (2022). Predicting the Remaining Service Life of Civil Airport Runway considering Reliability and Damage Accumulation. *Advances in Materials Science and Engineering*, 6494812. doi:10.1155/2022/6494812.
- [20] Modarres, A., & Shabani, H. (2015). Investigating the effect of aircraft impact loading on the longitudinal top-down crack propagation parameters in asphalt runway pavement using fracture mechanics. *Engineering Fracture Mechanics*, 150, 28–46. doi:10.1016/j.engfracmech.2015.10.024.
- [21] Moayedfar, R., & Sajjadifard, A. (2021). Prioritization of pavement restoration and maintenance strategies in airports using APMS technique. *International Journal of Pavement Research and Technology*, 14(3), 327–333. doi:10.1007/s42947-020-0244-4.
- [22] Babashamsi, P., Khahro, S. H., Omar, H. A., Al-Sabaei, A. M., Memon, A. M., Milad, A., Khan, M. I., Sutanto, M. H., & Yusoff, N. I. M. (2022). Perspective of Life-Cycle Cost Analysis and Risk Assessment for Airport Pavement in Delaying Preventive Maintenance. *Sustainability (Switzerland)*, 14(5), 2905. doi:10.3390/su14052905.
- [23] R., T., M.U., A., & M.M., R. (2013). Evaluating Functional and Structural Condition Based Maintenances of Airfield Pavements. *Civil Engineering Dimension*, 15(2), 71-80. doi:10.9744/ced.15.2.71-80.
- [24] Zhao, H., Ma, L., Tang, L., Li, M., & Du, H. (2018). Maintenance Assistant Decision-Making Model of Civil Airport Cement Pavements Based on Data Mining. *Journal of Tongji University*, 46(12), 1676-1682. doi:10.11908/j.issn.0253-374x.2018.12.009.
- [25] Wang, W., Wang, M., Li, H., Zhao, H., Wang, K., He, C., Wang, J., Zheng, S., & Chen, J. (2019). Pavement crack image acquisition methods and crack extraction algorithms: A review. *Journal of Traffic and Transportation Engineering (English Edition)*, 6(6), 535–556. doi:10.1016/j.jtte.2019.10.001.

- [26] Li, H. F., Wu, Z. L., Nie, J. J., Peng, B., & Gui, Z. C. (2020). Automatic crack detection algorithm for airport pavement based on depth image. *Jiaotong Yunshu Gongcheng Xuebao/Journal of Traffic and Transportation Engineering*, 20(6), 250–260. doi:10.19818/j.cnki.1671-1637.2020.06.022.
- [27] Jiang, L., Xie, Y., & Ren, T. (2020). A deep neural networks approach for pixel-level runway pavement crack segmentation using drone-captured images. *arXiv preprint, arXiv:2001.03257*. doi:10.48550/arXiv.2001.03257.
- [28] Li, B., Fu, M., & Li, Q. (2021). Runway Crack Detection Based on YOLOV5. 2021 IEEE 3rd International Conference on Civil Aviation Safety and Information Technology (ICCASIT), 1252–1255. doi:10.1109/iccasit53235.2021.9633666.
- [29] Liu, J., Liu, F., Zheng, C., Zhou, D., & Wang, L. (2022). Optimizing asphalt mix design through predicting the rut depth of asphalt pavement using machine learning. *Construction and Building Materials*, 356. doi:10.1016/j.conbuildmat.2022.129211.
- [30] Zhang, C., Nateghinia, E., Miranda-Moreno, L. F., & Sun, L. (2022). Pavement distress detection using convolutional neural network (CNN): A case study in Montreal, Canada. *International Journal of Transportation Science and Technology*, 11(2), 298–309. doi:10.1016/j.ijtst.2021.04.008.
- [31] Amhaz, R., Chambon, S., Idier, J., & Baltazart, V. (2016). Automatic Crack Detection on Two-Dimensional Pavement Images: An Algorithm Based on Minimal Path Selection. *IEEE Transactions on Intelligent Transportation Systems*, 17(10), 2718–2729. doi:10.1109/TITS.2015.2477675.
- [32] Ravi, R., Bullock, D., & Habib, A. (2020). Highway and airport runway pavement inspection using mobile LIDAR. *International Archives of the Photogrammetry, Remote Sensing and Spatial Information Sciences - ISPRS Archives*, 43(B1), 349–354. doi:10.5194/isprs-archives-XLIII-B1-2020-349-2020.
- [33] Cereceda, D., Medel-Vera, C., Ortiz, M., & Tramon, J. (2022). Roughness and condition prediction models for airfield pavements using digital image processing. *Automation in Construction*, 139, 139. doi:10.1016/j.autcon.2022.104325.
- [34] Kumar, P., & Sharma, M. (2022). Functional Condition Evaluation of Airfield Pavements Using Automated Road Survey System—A Case Study of a Small Sized Airport. *Road and Airfield Pavement Technology. Lecture Notes in Civil Engineering*, 193, Springer, Cham, Switzerland. doi:10.1007/978-3-030-87379-0\_13.
- [35] Pietersen, R., Beauregard, M., & Einstein, H. (2022). Automated method for airfield pavement condition index evaluations. *Automation in Construction*, 141, 104408. doi:10.1016/j.autcon.2022.104408.
- [36] Suh, Y. C., Park, D. Y., & Jeong, K. Y. (2002). Development of deterioration prediction models for airfield rigid pavements. *Transportation Research Record*, 1788(1788), 132–137. doi:10.3141/1788-17.
- [37] Yuan, J., & Mooney, M. A. (2003). Development of Adaptive Performance Models for Oklahoma Airfield Pavement Management System. *Transportation Research Record*, 1853(1853), 44–54. doi:10.3141/1853-06.
- [38] Tarefder, R. A., & Rahman, M. M. (2016). Development of system dynamic approaches to airport pavements maintenance. *Journal of Transportation Engineering*, 142(8), 04016027. doi:10.1061/(ASCE)TE.1943-5436.0000856.
- [39] Camarena Campos, K. A., & Flores Gonzales, L. (2018). Proposal of Numerical Model for Airport Pavement Management Purposes. *Proceedings of the 16th LACCEI International Multi-Conference for Engineering, Education, and Technology: "Innovation in Education and Inclusion."* doi:10.18687/laccei2018.1.1.417.
- [40] Saleh, N. F., Keshavarzi, B., Yousefi Rad, F., Mocelin, D., Elwardany, M., Castorena, C., Underwood, B. S., & Kim, Y. R. (2020). Effects of aging on asphalt mixture and pavement performance. *Construction and Building Materials*, 258, 258. doi:10.1016/j.conbuildmat.2020.120309.
- [41] Kwak, P. J., Kim, D. H., Kim, S. J., & Jeong, J. H. (2021). Development of a non-linear PCI model for homogeneous zones of concrete airport pavements. *Proceedings of the Institution of Civil Engineers: Transport*, 174(5), 305–319. doi:10.1680/jtran.18.00018.
- [42] Di Mascio, P., Ragnoli, A., Portas, S., & Santoni, M. (2021). Monitor activity for the implementation of a pavement—management system at cagliari airport. *Sustainability (Switzerland)*, 13(17), 9837. doi:10.3390/su13179837.
- [43] Ashtiani, A. Z. (2021). Application of Machine Learning Techniques to Pavement Performance Modeling. *DTFAC-15-D-00007*, Airport Engineering Division, Federal Aviation Administration, U.S. Department of Transportation, Washington, United States.
- [44] Ali, A. A., Esekbi, M. I., & Sreh, M. M. (2022). Predicting Pavement Condition Index Using Machine Learning Algorithms and Conventional Techniques. *Journal of Pure & Applied Sciences*, 21(4), 304–309. doi:10.51984/jopas.v21i4.2267.
- [45] Wibowo, A., Subagio, B. S., Rahman, H., & Frazila, and R. B. (2024). Evaluation of the Airport Pavement Condition Index in the Aircraft Lateral Wander Area. *International Journal of GEOMATE*, 27(122), 87–95. doi:10.21660/2024.122.g13151.